

Interaction-induced transparency for strong-coupling polaritons

Johannes Lang¹, Darrick E. Chang^{2,3}, and Francesco Piazza⁴

¹*Physik Department, Technische Universität München, 85747 Garching, Germany*

²*ICFO-Institut de Ciències Fotoniques, The Barcelona Institute of Science and Technology, 08860 Castelldefels (Barcelona), Spain*

³*ICREA-Institució Catalana de Recerca i Estudis Avançats, 08015 Barcelona, Spain and*

⁴*Max-Planck-Institut für Physik komplexer Systeme, 01187 Dresden, Germany*

The propagation of light in strongly coupled atomic media takes place through the formation of polaritons - hybrid quasi-particles resulting from a superposition of an atomic and a photonic excitation. Here we consider the propagation under the condition of electromagnetically-induced transparency and show that a novel many-body phenomenon can appear due to strong, dissipative interactions between the polaritons. Upon increasing the photon-pump strength, we find a first-order transition between an opaque phase with strongly broadened polaritons and a transparent phase where a long-lived polariton branch with highly tunable occupation emerges. Across this non-equilibrium phase transition, the transparency window is reconstructed via nonlinear interference effects induced by the dissipative polariton interactions. Our predictions are based on a systematic diagrammatic expansion of the non-equilibrium Dyson equations which is quantitatively valid, even in the non-perturbative regime of large single-atom cooperativities, provided the polariton interactions are sufficiently long ranged. Such a regime can be reached in photonic crystal waveguides thanks to the tunability of interactions, allowing to observe the interaction-induced-transparency transition even at low polariton densities.

Introduction.— Slow light in coherent media via electromagnetically induced transparency (EIT) [1] has become a cornerstone of quantum optics, allowing for instance to store and even shape individual photons [2–4]. EIT is a linear optical phenomenon resulting from destructive interference between dipole-excitation pathways. Combined with strong atomic Rydberg interactions, EIT has also turned out to be a key ingredient in achieving single-photon non-linearities [5, 6], potentially allowing for efficient transmission, manipulation, and storage of quantum information [7]. On the other hand, single-photon nonlinearities pave the way for the study of novel quantum many-body phenomena with strongly interacting photons [5].

In this letter, we consider EIT polaritons, mixing a set of electromagnetic modes with internal atomic excitations, in the presence of strong, partially dissipative interactions. The latter typically destroy the EIT window [6, 8]. However, under certain conditions, at a threshold value of the rate at which photons are injected into the system, we find a first-order phase transition in the driven/dissipative steady-state, separating an opaque phase (OP) with a low density of strongly broadened polaritons from a transparent phase (TP), characterized by the existence of a long-lived polariton branch with a high spectral density. The novelty and peculiarity of this transition resides in the fact that in the TP the transparency window is reconstructed via nonlinear interference effects induced by the dissipative interactions, in a process that we name interaction-induced transparency (IIT). The first-order transition is accompanied by a bistable region where the OP and TP coexist.

We employ a diagrammatic expansion of the Dyson equations for the non-equilibrium response and correla-

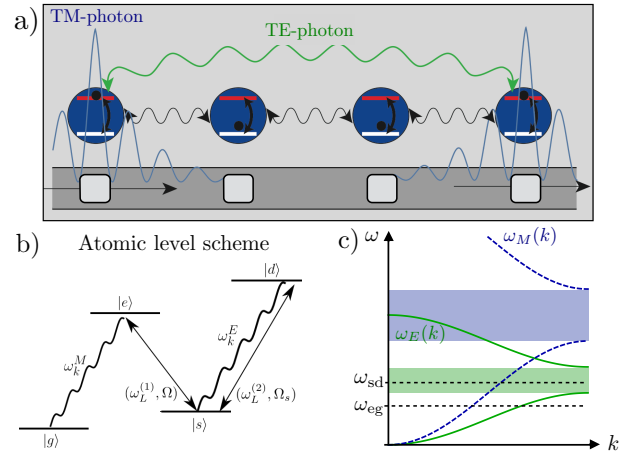


FIG. 1. a) Proposed realization of IIT: A chain of atoms are fixed in a periodic arrangement in the evanescent field of the PCW. The atoms interact via internal electronic transitions (shown in b)) with two continua of photonic modes of the PCW with different transverse polarization. Panel c) shows where the atomic transitions lie relative to the band structure of both polarizations.

tion functions. This novel approach, described in detail elsewhere [9], allows for quantitative predictions even in the non-perturbative regime of large single-atom cooperativities (where IIT takes place), provided the polariton interactions are sufficiently long ranged.

We consider in detail a possible implementation of IIT with photonic crystal waveguides (PCWs). There, the polaritonic excitations can be made to strongly interact via localized, non-propagating photons within a bandgap

(see also Fig. 1). The engineered photon band-structure potentially allows to control not only their dispersion but also both the strength and the range of interactions [10–12], as well as the coupling with the environment [13].

Model and approach.— We consider an array of four-level atoms as illustrated in Fig. 1(b). The $|g\rangle - |e\rangle$ transition between the atomic ground and excited states is coupled to guided photons (e.g. a Bloch band of transverse magnetic polarization in a photonic crystal waveguide) with dispersion relation $\omega_M(k)$, while $|e\rangle$ is coupled to an additional metastable state $|s\rangle$ via a coherent control field with Rabi frequency Ω . In such a configuration the propagating photons, that are near-resonant with the $|g\rangle - |e\rangle$ transition, hybridize with atomic excitations to $|s\rangle$ which can lead to EIT [2]. In particular, the destructive interference between the $|g\rangle \rightarrow |e\rangle$ and $|g\rangle \rightarrow |e\rangle \rightarrow |s\rangle \rightarrow |e\rangle$ excitation pathways suppresses population of $|e\rangle$ and the associated spontaneous emission and dissipation of the propagating photons within a narrow frequency and momentum window. The polaritons associated with this otherwise linear optical effect can be made to interact strongly by coupling $|s\rangle$ to a second excited state $|d\rangle$ by means of a second control field of Rabi frequency Ω_s . We assume that the $|s\rangle - |d\rangle$ transition is slightly off-resonant with respect to a separate photonic band with dispersion relation $\omega_E(k)$. As illustrated in Fig. 1 in a PCW the transition can be engineered to lie within the bandgap of e.g. the transverse electrically polarized photons or, alternatively, below the mass gap of photons in tapered fibers. An atomic excitation $|d\rangle$ is then unable to spontaneously emit a guided photon due to the absence of resonant modes. Instead, a photon becomes “bound” around the atomic excitation, which facilitates strong interactions with nearby atoms [14]. Due to the finite life times of both state $|d\rangle$ and the E photon, these are in fact mostly dissipative. Furthermore the atoms are assumed to be fixed in a periodic arrangement, which can be achieved using tweezers [15, 16] or the evanescent field of PCWs [17]. We will consider the linear regime of small atomic excitation densities, where we can replace spin operators with bosonic creation/annihilation operators $\hat{\sigma}_{ee} \rightarrow \hat{a}_e^\dagger \hat{a}_e$, $\hat{\sigma}_{eg} \rightarrow \hat{a}_e^\dagger \hat{a}_g$, and similarly for the other atomic transitions. The Hamiltonian of the system is given by a free part (setting $\hbar = 1$)

$$\hat{H}_0 = \sum_z \sum_{j=e,s,d} \omega_j \hat{a}_j^\dagger(z) \hat{a}_j(z) + \int_k \sum_{j=M,E} \omega_j(k) \hat{a}_j^\dagger(k) \hat{a}_j(k)$$

with dispersions $\omega_E(k) \simeq \omega_E(k_0) + \alpha_E(k - k_0)^2$ and $\omega_M(k)$, where the precise form of the latter depends on the physical realization and is of no qualitative relevance for the following results. Additionally, the atoms interact

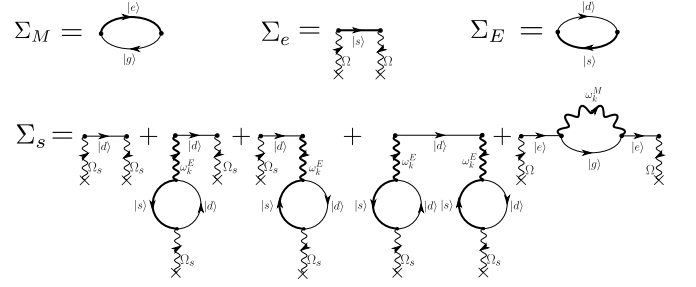


FIG. 2. Self-consistent Hartree diagrammatic approach to the computation of self-energies for the magnetically/electrically polarized photons $\Sigma_{M/E}$ and the atoms in the metastable state Σ_s . Internal solid/wiggled lines represent atom/photon propagators while wiggled legs ending in a cross indicate insertions of a static laser field. Bold lines correspond to propagators including self-energy corrections, which implies a self-consistent treatment. In order to account for the fact that an atom can be excited only once, all diagrams where the same atoms appears more than once in the same state must be removed [9].

with laser and guided photons via

$$\hat{H}_{\text{int}} = \sum_z \left[\Omega e^{-i\omega_L^{(1)}t} \hat{a}_e^\dagger(z) \hat{a}_s(z) + \Omega_s e^{-i\omega_L^{(2)}t} \hat{a}_d^\dagger(z) \hat{a}_s(z) \right. \\ \left. + \sum_{j=M,E} \int_k g_j \hat{a}_j(k) e^{ikz} u_k^j(z) \hat{a}_{\text{exc}(j)}^\dagger(z) \hat{a}_{\text{gs}(j)}(z) + h.c. \right] \quad (1)$$

with the notation $\text{gs}(M/E) = g/s$, $\text{exc}(M/E) = e/d$, and where \sum_z runs over the sites of the atomic lattice and $u_k^{M/E}(z)$ represents the periodic part of the Bloch functions of either polarization at quasi-momentum k . We use the standard convention $\sum_z e^{ikz} = 2\pi\delta(k)$ with lattice constant $a = 1$ and $\int_k = \int_{-\pi}^{\pi} \frac{dk}{2\pi}$ for the integration over quasi-momenta. The incoherent dynamics is described by

$$\left(\sum_{j=e,d,s} \gamma_j \mathcal{D}[\hat{a}_j(z)] + L \int_k (\kappa_s \mathcal{P}[\hat{a}_M(k)] + \sum_{j=M,E} \kappa_j \mathcal{D}[\hat{a}_j(k)]) \right) \hat{\rho}$$

with the dissipator $\mathcal{D}[\hat{L}]\hat{\rho} = -(\{\hat{L}^\dagger \hat{L}, \hat{\rho}\} - 2\hat{L} \hat{\rho} \hat{L}^\dagger)/2$ describing the spontaneous decay of the excited atomic states plus the photon losses out of the guided modes, and the pump $\mathcal{P}[\hat{L}]\hat{\rho} = -(\{\hat{L} \hat{L}^\dagger + \hat{L}^\dagger \hat{L}, \hat{\rho}\} - 2\hat{L}^\dagger \hat{\rho} \hat{L} - 2\hat{L} \hat{\rho} \hat{L}^\dagger)/2$ homogeneously injecting M-photons into the waveguide. The incoherent pump results from coupling with a reservoir and therefore cannot generate an inversion in the $k = 0$ mode, which excludes the phenomenon of polariton condensation [18, 19].

Since we are interested in the steady state of this quantum driven/dissipative interacting system in the thermodynamic limit, we employ the Keldysh non-equilibrium functional integral formalism [20–22] to compute single-particle Green’s functions (or propagators). Due to the

absence of thermal equilibrium, there are in principle two independent propagators, the retarded $i(G_j^R(x, x')) = \theta(t-t')\langle[\hat{a}_j(x), \hat{a}_j^\dagger(x')]\rangle$, and the Keldysh Green's function $i(G_j^K(x, x')) = \langle\{\hat{a}_j(x), \hat{a}_j^\dagger(x')\}\rangle$ with $j = g, e, s, d, E, M$ labeling the degree of freedom and $x = z, t$ being the space-time coordinate. These two propagators satisfy two coupled non-equilibrium Dyson equations, for which we developed a controlled diagrammatic treatment of the interaction processes that is described in detail elsewhere [9].

Here we limit ourselves to introducing the self-consistent Hartree (SCH) theory illustrated diagrammatically in Fig. 2 and formally in the Supplemental Material. This SCH theory is the simplest set of diagrams giving rise to IIT, allowing for the clearest illustration of the phenomenon. As shown in [9], the SCH approach can be extended in a controlled manner (by including a few more diagrams) to become quantitative even in the non-perturbative regime of large single-atom cooperativities considered below. The M -photon self-energy Σ_M^R of Fig. 2, is the susceptibility (or polarization function) describing the modified propagation in the atomic medium. The contribution to Σ_M involving a bare e -propagator adds up with the one involving the insertion of Σ_e , which corresponds to the interference of pathways underlying EIT. We include the modified propagation due to the medium also for the E -photons through the self-energy Σ_E . Finally, the interactions between s -atoms mediated by E -photons are taken into account at the Hartree level by the first four diagrams in Σ_s . Since the level s is not driven, those diagrams vanish unless we dress the s propagator with the last diagram, which creates a finite occupation in $|s\rangle$ with the help of an M -photon. In a diagrammatic loop expansion, this means that the first non-vanishing correction to the EIT propagation of the M -photons appears at the 3-loop level. Our approach is non-perturbative in two ways: i) the Dyson equation implies a resummation of an infinite number of self-energy insertions, which is for instance needed to describe EIT; ii) the self-energies contain bold s, M and E propagators, indicating a self-consistent treatment. In particular, this allows to account for the fact that the E -photon-mediated interactions are screened due to polarization effects and that the population transfer into the interacting $|s\rangle$ state via the M -photons takes place only within the EIT transparency window.

The SCH approach of Fig. 2 captures the energy-shift and modified damping of the atoms in state $|s\rangle$ due to the E -photon mediated interactions, but neglects the scattering processes involving energy and momentum transfer.

As explained in [9], this approach is justified in the regime of a small single-atom cooperativity $C_E = g_E^2/(\kappa_E \gamma_d L_E) \ll 1$, where L_E is the effective (i.e. including polarization effects) propagation range of the E -photons in units of the atom spacing a . L_E also cor-

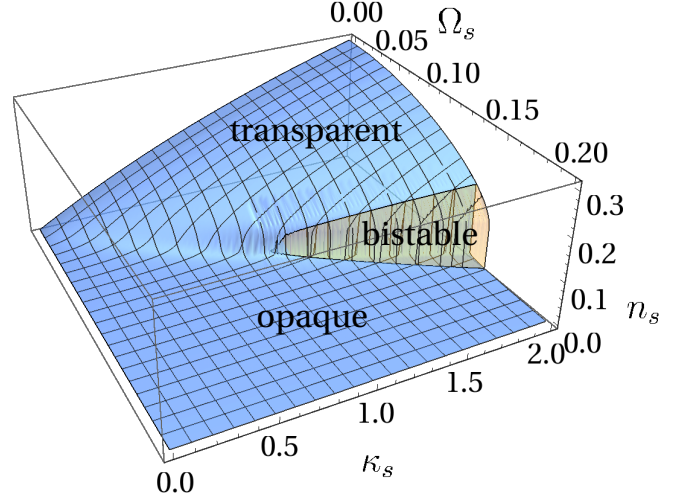


FIG. 3. Excitation density in the atomic state s . The yellow(blue) surface corresponds to a system initialized in the “transparent”(“opaque”) phase with vanishing(large) values of κ_s . Parameters are $\kappa_0 = 2$, $\kappa_s = 1$, $\omega_0 = \Delta_s \equiv \omega_s + \omega_L^{(1)} - \omega_e = \Delta_d \equiv \omega_d - \omega_s - \omega_L^{(2)} = n_V = 0$, $g_P = g_E = 10$, $\kappa_P = 0.5$, $\gamma_d = 1$, $\kappa_E = 5$, $\Omega = 0.2$, $\omega_E(k) = \omega_L^{(2)} - 100k^2$ and $\omega_P(k) = -50 \cos k - \omega_e$ in units where $\gamma_e = 1$.

responds to the effective interaction range between the atoms in state $|s\rangle$, which when $\kappa_E \gg \omega_L^{(2)} - \omega_E(0)$ simply reads $L_E \simeq \sqrt{\alpha_E/\kappa_E}$. On the other hand, inside the transparency window M -photons propagate essentially freely, so that $L_M \simeq v_M/\kappa_M$, where we assumed a linear dispersion with slope v_M inside the EIT window (see Fig. 4). Note that our approach does not require a small single-atom cooperativity $C_M = g_M^2/(\kappa_M \gamma_e L_M)$. Therefore, the strong coupling regime, where

$$pL_EC_EC_M \frac{\Omega_s^2}{\Omega^2} \gg 1, \quad (2)$$

with the pump ratio $p = \kappa_s/\kappa_M$ fixing the density of excitations, can be described faithfully. This is necessary for interaction-induced shifts to become important, so that non-perturbative effects like IIT can appear [9].

Results.— In the steady-state the system is translation invariant in both time and space. This allows to write the retarded M -photon propagator in the most general form (within our SCH approach) as [23] $G_M^R(\omega, k) = (\omega - \omega_M(k) - \Sigma_M^R(\omega, k) + i\kappa_M/2)^{-1}$ with the self-energies of Fig. 2 given by

$$\begin{aligned} \Sigma_M^R(\omega, k) &= \frac{g_M^2 |u_k^M(0)|^2 (1 - n_V)}{\omega - \omega_e - \frac{\Omega^2}{\omega - \omega_s - \omega_L^{(1)} - \Sigma_s^R(\omega - \omega_L^{(1)})} + i\gamma_e/2} \\ \Sigma_s^R(\omega) &= \frac{(\Omega_s^{\text{eff}})^2}{\omega - \omega_d + \omega_L^{(2)} + i\gamma_d/2} \end{aligned} \quad (3)$$

where n_V is the average number of defect-atoms with respect to unit filling of the photonic crystal. The stan-

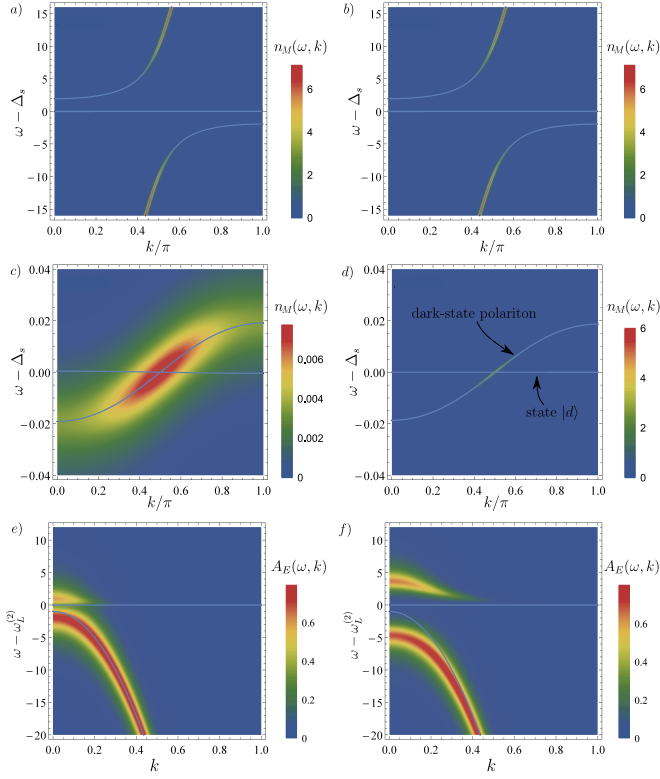


FIG. 4. Comparison between the opaque (left) and transparent (right) solution. Top row: M-photon occupation in frequency-momentum space. Solid blue lines correspond to the dispersion curve of the polariton branches. Mid-row: enlarged view of the dark-state polariton branch. Bottom row: spectral function of the E-photons. Solid lines correspond to the bare E-photon dispersion (inverted parabola) and the resonance frequency of the $s - d$ transition (horizontal line). The parameters are the same as in Fig. 3 at the bistable point $\Omega_s = 0.14$ and $\kappa_s = 2$.

dard non-interacting EIT corresponds to setting $\Omega_s^{\text{eff}} = 0$ in Eq. (5). The (imaginary) poles of G_M^R yield all polariton branches. The effect of the E-photon mediated interactions in the steady state within our SCH approach is parametrized by the single real constant $\Omega_s^{\text{eff}} = \Omega_s |1 + \chi|$. The latter satisfies however a non-trivial integral equation given in the Supplemental Material and represented diagrammatically in Fig. 2.

The phase diagram as a function of the M-photon pump κ_s and $s - d$ drive Ω_s is shown in Fig. 3. We find two possible steady-state phases: i) an “opaque” phase characterized by a small atomic excitation density n_s and ii) a “transparent” phase exhibiting instead a much larger n_s . Those two phases are separated by a first order phase transition that includes a bistable region and terminates in a bi-critical point where the transition is continuous.

More insight into the properties of the opaque and transparent phases are obtained by examining the frequency- and momentum-resolved occupation $n_M(\omega, k)$ shown in Fig. 4, defined by $\int_{k, \omega} n_M(\omega, k) = n_M$. In

addition to the three polariton branches of the non-interacting EIT, a fourth branch emerges as a consequence of the coupling to the level d (see Fig. 1). Since the coupling is weak it is an almost non-dispersive flat band at $\omega \approx \omega_d + \omega_L^{(1)} - \omega_L^{(2)}$.

In the opaque phase, the intensity is almost exclusively distributed on the two outer branches, which are far-off resonant with respect to the atomic transitions and therefore are not influenced by the atomic medium. The two central branches are essentially empty i.e. no sign of the EIT window on the dark-state polariton branch (upper branch within the central pair in Fig. 4) is left. The latter is destroyed by coupling the metastable state $|s\rangle$ to the excited state $|d\rangle$, introducing an additional decay channel that is eventually inherited by the dark-state polariton. Correspondingly, the additional polariton branch resulting from the coupling to the d -level hybridizes with the dark-state polariton.

In the transparent phase on the other hand the intensity is concentrated within a very sharp region around a specific wavenumber k_{EIT} of the dark-state polariton branch. This means that in the phase transition the system has reconstructed the transparency window. In the original non-interacting EIT effect, the window is formed due to the destructive interference between the two excitation pathways corresponding to the two diagrams for Σ_M in Fig. 2. In the IIT effect, the window is also reconstructed via destructive interference, this time between the four different excitation pathways involving the state $|d\rangle$ and corresponding to the first four diagrams contributing to Σ_s in Fig. 2. Other than in the non-interacting EIT, the interfering pathways involve the E-photons i.e. interactions between polaritons, which renders IIT intrinsically nonlinear. In the lossy system this implies that IIT takes place through a first-order phase transition showing bistability. The transparency window is reconstructed at a slightly different position with respect to the non-interacting case with the EIT-wavenumber still being very well approximated by $\omega_M(k_{\text{EIT}}) = \omega_s + \omega_L^{(1)} - \omega_g$. The destructive interference between the four pathways is most efficient if the self-energy of the E-photons $\Sigma_E^R(\omega_L^{(2)} + \omega_s)$ becomes purely imaginary, corresponding to strong screening between E-photons and the external laser. This indicates that IIT is a dissipative many-body effect only accessible to systems far from thermal equilibrium.

The destruction of the transparency window in the opaque phase via coupling to a lossy state is an effect analogous to the one employed to build an optical switch in [8], whereby any two-photon state becomes strongly suppressed. If one uses a lossy state to induce interactions between atoms in the metastable state, the IIT additionally enables to reconstruct transparency at a tunable photon number.

The E-photons mediating the interactions between the

atoms also show drastic differences between the opaque and transparent phase. As opposed to the M -photons, E -photons are not driven and can only be excited by atoms in the d level. The latter can be occupied only via laser transitions from the s level, which in turn can be populated via absorption of M -photons. Therefore, the occupation of the electrically polarized mode is suppressed by $1/L_M$ and thus typically small for realistic parameters. It is therefore more instructive to analyze the spectral function, defined as $A_E(\omega, k) = -2\Im G_E^R(\omega, k)$, which is normalized to 1 and accessible for instance by combining the waveguide output with a reference field on a beam-splitter [24]. $A_E(\omega, k)$ is shown in the bottom row of Fig. 4. In the opaque phase the spectral weight is mostly on the bare dispersion curve, with a width set by the losses κ_E . This is caused by the low number of atoms in state s , which makes the modification Σ_E of the photon-propagation due to the medium negligible. On the other hand, in the transparent phase we see that the bare E -photon branch hybridizes with the atomic $s - d$ excitation. In addition, in the momentum region close to the dispersion maximum, spectral weight is transferred from the photon-like branch to the atom-like branch. This screening effect is quantitatively important and reduces the strength of the E -photon-mediated interactions for polaritons in the transparency window. Adiabatic elimination of the bare E -photons would therefore largely overestimate the bright region in the phase diagram.

Realization.— According to the condition (2), the emergence of IIT requires strong atom-light interactions. Fortunately, this requirement is met for parameters that are expected to become experimentally viable in PCWs in the near future [14], namely $\gamma_{e,d} \sim 10\text{MHz}$, $g_{M,E} \sim 10^3\gamma_e$, $J_M \sim 10^7\gamma_e$, $\alpha_E \sim 10^6\gamma_e$ and $\kappa_{M,E} \sim 10\gamma_e$, for which our approach indeed predicts the existence of a IIT transition. Because of the highly tunable photon dispersions in PCWs this will likely be possible with $C_E \lesssim 1$, where our theory becomes quantitatively valid. It is also worth mentioning that the additional diagrams that need to be added to the ones in Fig. 2 in order to render our predictions fully quantitative actually enhance the IIT-effect, which results in a parametrically larger bistable region [9].

As for the above realistic parameters the relative width of the EIT window becomes extremely small, in Figs. 3,4 we have, for illustrative purposes, chosen a different set that however still satisfies $J_M > g_{M,E} > \kappa_{M,E} > \gamma_{e,d}$.

Conclusions.— We introduced the phenomenon of interaction-induced transparency (IIT), which is characterized by the appearance of a transparency window for strongly interacting polaritons due to nonlinear interference effects. In the context of nonlinear quantum optics, IIT constitutes a novel, genuine quantum many-body effect. From the more fundamental perspective of many-body physics, the IIT phenomenon is a non-equilibrium

phase transition in the driven-dissipative steady state which has no analogue so far in condensed matter, as it stems from the dissipative and retarded nature of the interactions between polaritons. It would be also interesting to determine whether IIT belongs to the recently proposed scenario of dark-state phase transitions [25].

Future directions could also involve the study of the role played by IIT in pump-probe experiments, where a light pulse is locally injected and its transient dynamics is investigated.

We are grateful to Wilhelm Zwerger for careful reading of the manuscript. DC acknowledges support from ERC Starting Grant FOQAL, MINECO Plan Nacional Grant CANS, MINECO Severo Ochoa Grant No. SEV-2015-0522, CERCA Programme/Generalitat de Catalunya, and Fundacio Privada Cellex.

-
- [1] M. Fleischhauer, A. Imamoglu, and J. P. Marangos, *Rev. Mod. Phys.*, **77**, 633 (2005).
 - [2] M. Fleischhauer and M. D. Lukin, *Phys. Rev. A*, **65**, 022314 (2002).
 - [3] P. Vernaz-Gris, K. Huang, M. Cao, A. S. Sheremet, and J. Laurat, *Nature Communications*, **9**, 363 (2018), ISSN 2041-1723.
 - [4] B. C. Pursley, S. G. Carter, M. K. Yakes, A. S. Bracker, and D. Gammon, *Nature Communications*, **9**, 115 (2018), ISSN 2041-1723.
 - [5] D. E. Chang, V. Vuletic, and M. D. Lukin, *Nat Photon*, **8**, 685 (2014).
 - [6] O. Firstenberg, C. S. Adams, and S. Hofferberth, *Journal of Physics B: Atomic, Molecular and Optical Physics*, **49**, 152003 (2016).
 - [7] H. J. Kimble, *Nature*, **453**, 1023 (2008).
 - [8] M. Bajcsy, S. Hofferberth, V. Balic, T. Peyronel, M. Hafezi, A. S. Zibrov, V. Vuletic, and M. D. Lukin, *Phys. Rev. Lett.*, **102**, 203902 (2009).
 - [9] J. Lang, D. Chang, and F. Piazza, *arXiv preprint arXiv: (2018)*.
 - [10] J. S. Douglas, H. Habibian, C.-L. Hung, G. A. V., K. H. J., and D. E. Chang, *Nat Photon*, **9**, 326 (2015), ISSN 1749-4885.
 - [11] J. S. Douglas, T. Caneva, and D. E. Chang, *Phys. Rev. X*, **6**, 031017 (2016).
 - [12] T. Shi, D. E. Chang, and J. I. Cirac, *Physical Review A*, **92**, 053834 (2015).
 - [13] A. Asenjo-Garcia, M. Moreno-Cardoner, A. Albrecht, H. J. Kimble, and D. E. Chang, *Phys. Rev. X*, **7**, 031024 (2017).
 - [14] A. Goban, C. L. Hung, S. P. Yu, J. D. Hood, J. A. Muniz, J. H. Lee, M. J. Martin, A. C. McClung, K. S. Choi, D. E. Chang, O. Painter, and H. J. Kimble, *Nat Commun*, **5** (2014).
 - [15] J. D. Thompson, T. G. Tiecke, N. P. de Leon, J. Feist, A. V. Akimov, M. Gullans, A. S. Zibrov, V. Vuletić, and M. D. Lukin, *Science*, **340**, 1202 (2013), ISSN 0036-8075, <http://science.sciencemag.org/content/340/6137/1202.full.pdf>.
 - [16] M. Endres, H. Bernien, A. Keesling, H. Levine, E. R. Anschuetz, A. Krajenbrink, C. Senko, V. Vuletic,

- M. Greiner, and M. D. Lukin, (2016), ISSN 0036-8075, doi:10.1126/science.aah3752.
- [17] C.-L. Hung, S. M. Meenehan, D. E. Chang, O. Painter, and H. J. Kimble, *New Journal of Physics*, **15**, 083026 (2013).
- [18] I. Carusotto and C. Ciuti, *Rev. Mod. Phys.*, **85**, 299 (2013).
- [19] L. M. Sieberer, S. D. Huber, E. Altman, and S. Diehl, *Phys. Rev. B*, **89**, 134310 (2014).
- [20] A. Kamenev, *Field Theory of Non-Equilibrium Systems* (Cambridge University Press, 2011) ISBN 9781139500296.
- [21] L. M. Sieberer, M. Buchhold, and S. Diehl, *Reports on Progress in Physics*, **79**, 096001 (2016).
- [22] J. Lang and F. Piazza, *Phys. Rev. A*, **94**, 033628 (2016).
- [23] See Supplemental Material.
- [24] M. Buchhold, P. Strack, S. Sachdev, and S. Diehl, *Phys. Rev. A*, **87**, 063622 (2013).
- [25] D. Roscher, S. Diehl, and M. Buchhold, arXiv preprint arXiv:1803.08514 (2018).

SUPPLEMENTAL MATERIAL

The mathematical structure of the SCH approach

In the diagrammatic representation of our SCH approach, every expression in Fig. 2, corresponds to a propagator (or Green's function), which in the Keldysh framework can be either the retarded G^R , advanced G^A or the Keldysh G^K propagator. However retarded and advanced Green's functions are not independent and thus, in general every diagram can generate two self-energy contributions $\Sigma^{R,K}$. In turn, the internal lines can either be G^R or G^K , provided the contraction is compatible with the interaction vertex and causality is guaranteed. We skip here all the details of the derivation of the expressions corresponding to the diagrams in Fig. 2, which are given in [9]. We also specify to the translation invariant case discussed in the main text, where the photon propagators depend on frequency and only a single momentum, while the atom propagators depend solely on the frequency. The M -photon propagator reads:

$$\begin{aligned} G_M^R(\omega, k) &= [G_M^A(\omega)]^* = \frac{1}{\omega - \omega_M(k) - \Sigma_M^R(\omega, k) + i\kappa_M/2} \\ G_M^K(\omega, k) &= G_M^R(\omega, k) (\Sigma_M^K(\omega, k) - i\kappa_M - 2i\kappa_s) G_M^A(\omega, k), \end{aligned} \quad (4)$$

with

$$\begin{aligned} \Sigma_M^R(\omega, k) &= \frac{g_M^2 |u_k^M(0)|^2 (1 - n_V)}{\omega - \omega_e - \Omega^2 \tilde{G}_s^R(\omega + \omega_L^{(1)}) + i\gamma_e/2} \\ \Sigma_M^K(\omega, k) &= 2i\text{Im}\Sigma_M^R(\omega, k) \end{aligned} \quad (5)$$

where $1 - n_V$ is the atom filling factor in the photonic crystal waveguide and the effective s -atom propagator

$$\tilde{G}_s^R(\omega) = [\tilde{G}_s^A(\omega)]^* = \frac{1}{\omega - \omega_s - \tilde{\Sigma}_s^R(\omega) + i0/2} \quad (6)$$

with

$$\tilde{\Sigma}_s^R(\omega) = \frac{(\Omega_s^{\text{eff}})^2}{\omega + \omega_L^{(2)} - \omega_d + i\gamma_d/2}. \quad (7)$$

Here $\Omega_s^{\text{eff}} = \Omega_s^2 (1 + \chi)^2$ is the effective Rabi amplitude modified by the E photons, which we parametrize by the dimensionless, complex constant χ . Note that this construction of Σ_M^R takes into account the fact that we have to exclude all diagrams where the same atoms appear in the same state twice. This is achieved by removing the last diagram for Σ_s in Fig. 2 whenever s atoms appear inside the polarization loop of the M -photons. For the same reason, in the first four diagrams for Σ_s , the internal s -propagators are allowed to contain only the last diagram as self-energy insertion. This defines a second type of s -propagator:

$$\tilde{\tilde{G}}_s^R(\omega) = [\tilde{\tilde{G}}_s^A(\omega)]^* = \frac{1}{\omega - \omega_s - \tilde{\tilde{\Sigma}}_s^R(\omega) + i0^+/2} \quad (8)$$

with

$$\tilde{\tilde{\Sigma}}_s^R(\omega) = \frac{\Omega^2}{\omega - \omega_e + \omega_L^{(1)} - \Sigma_e^R(\omega + \omega_L^{(1)}) + i\gamma_e/2} \quad (9)$$

and

$$\begin{aligned}\tilde{\Sigma}_s^K(\omega) &= 2i\text{Im}\tilde{\Sigma}_s^R(\omega) + \delta\tilde{\Sigma}_s^K(\omega) \\ \delta\tilde{\Sigma}_s^K(\omega) &= \frac{\Omega^2 \left(\Sigma_e^K(\omega + \omega_L^{(1)}) - 2i\text{Im}\Sigma_e^R(\omega + \omega_L^{(1)}) \right)}{\left(\omega - \omega_e + \omega_L^{(1)} - \text{Re}\Sigma_e^R(\omega + \omega_L^{(1)}) \right)^2 + \left(\gamma_e/2 - \text{Im}\Sigma_e^R(\omega + \omega_L^{(1)}) \right)^2},\end{aligned}\quad (10)$$

where

$$\begin{aligned}\Sigma_e^R(\omega) &= -\sum_n \int \frac{dk}{2\pi} g_M^2 \frac{\kappa_s}{2\text{Im}(\omega_n(k))} \frac{1}{\omega - \omega_n(k) + i0^+/2} \frac{f(\omega_n(k))f^*(\omega_n^*(k))}{\prod_{m \neq n} (\omega_n(k) - \omega_m(k))(\omega_n(k) - \omega_m^*(k))} |u_k^M(0)|^2 \\ &\quad + \int \frac{dk}{2\pi} \frac{1}{2} g_M^2 (4 - 2n_V) |u_k^M(0)|^2 G_M^R(\omega + i0^+/2, k) \\ \Sigma_e^K(\omega) &= 2i\text{Im}\Sigma_e^R(\omega) - i\kappa_s \int \frac{dk}{2\pi} g_M^2 (2 - 2n_V) |u_k^M(0)|^2 G_M^R(\omega, k) G_M^A(\omega, k),\end{aligned}\quad (11)$$

where $n \in \{1, 2, 3, 4\}$, $\omega_n(k)$ are the poles of $G_M^K(\omega, k)$ and

$$\begin{aligned}f(\omega) &= (\omega - \omega_e + i\gamma_e/2)(\omega - \omega_s - \omega_L^{(1)} + i0^+/2)(\omega - \omega_d - \omega_L^{(1)} + \omega_L^{(2)} + i\gamma_d/2) \\ &\quad - \Omega^2(\omega - \omega_d - \omega_L^{(1)} + \omega_L^{(2)} + i\gamma_d/2) - (\Omega_s^{\text{eff}})^2(\omega - \omega_e + i\gamma_e/2).\end{aligned}\quad (12)$$

The constant χ in the effective Rabi amplitude $\Omega_s^{\text{eff}} = \Omega_s|1 + \chi|$ is then to be determined self-consistently. The corresponding equation is

$$\chi = \frac{\Sigma_E^R(\omega_L^{(2)})}{\omega_L^{(2)} - \omega_E(0) - \Sigma_E^R(\omega_L^{(2)}) + i\kappa_E/2},\quad (13)$$

where the E -photon self-energy reads

$$\Sigma_E^R(\omega) = \frac{i}{2} \int \frac{d\omega'}{2\pi} g_E^2 \tilde{G}_s^R(\omega') \tilde{G}_s^A(\omega') \delta\tilde{\Sigma}_s^K(\omega') \frac{1}{\omega' + \omega - \omega_d + i\gamma_d/2}.\quad (14)$$

The latter describes the modification of the E -photon propagation, and thus of the light-mediated atom-atom interactions, due to the medium. The photon propagator is then given by

$$\begin{aligned}G_E^R(\omega, k) &= [G_E^A(\omega)]^* = \frac{1}{\omega - \omega_E(k) - \Sigma_E^R(\omega, k) + i\kappa_E/2} \\ G_E^K(\omega, k) &= G_E^R(\omega, k) (\Sigma_E^K(\omega, k) - i\kappa_E) G_E^A(\omega, k),\end{aligned}\quad (15)$$

with

$$\Sigma_E^K(\omega, k) = 2i\text{Im}\Sigma_E^R(\omega, k).\quad (16)$$